Supporting Information

The aggregation-caused quenching effect and fluorescence enhancement features of ZIF-90 and their feasibility for the detection and imaging of ATP in cells

Jing-Hao Fu[a], Xuan Wang[b], Qi-He Xia[a], Zeng-Ping Chen[*, a], Ping-Fan Shen [a], Yao Chen[*, a, c] and Ru-Qin Yu[a]

a. State Key Laboratory of Chemo/Biosensing and Chemometrics, College of Chemistry and Chemical Engineering, Hunan University, Changsha, Hunan 410082, P. R. China.

b. Shanghai Yanlu Maman Technology Co., Ltd., Shanghai, 200030, P. R. China.

c. Hunan Key Lab of Biomedical Materials and Devices, College of Life Sciences and Chemistry, Hunan University of Technology, Zhuzhou, 412008, PR China.

* To whom correspondence should be addressed.

E-mail: zpchen@hnu.edu.cn (Z.P. Chen), chenyao717@hnu.edu.cn (Y. Chen).

Experimental Section

Materials and regents

Adenosine triphosphate (ATP), adenosine monophosphate (AMP), adenosine diphosphate (ADP), pyrophosphoric acid (PPi), trisodium phosphate (TSP), and $Zn(CH_3COOH)_2 \cdot 2H_2O$ were purchased from Aladdin Reagent Ltd. (Shanghai, China). Imidazolate-2-carboxyaldehyde (2-ICA), methyl alcohol (anhydrous, ≥99.8%) were obtained from Shanghai Macklin Biochemical Technology Co., Ltd. (Shanghai, China). 2'-(4-ethoxyphenyl)-5-(4-methylpiperazin-1-yl)-2,5'-bibenzimidazole (Hoechst 33342) was supplied by Beyotime (Shanghai, China). All oligonucleotides (Table S2) used in this contribution were synthesized and purified by Sangon Biological Engineering Technology (Shanghai, China). Unless otherwise stated, all the reagents were analytical grade and used as received without further purification. All aqueous solutions were prepared with ultra-pure water (≥18.25 MΩ·cm) produced by a Millipore Milli-Q water purification system (Billerica, MA, USA).

Apparatus

A Hitachi S-3400N scanning electron microscope (SEM) equipped with an ESCALab220i-XL energy-dispersive X-ray (EDX) spectrometer (Hitachi Corporation, Japan) was used to characterize the structures of nanoparticles. Dynamic light scattering (DLS) and surface charge (zeta potential) of nanoparticles were analyzed using a Malvern Zetasizer Nano ZS90 (Malvern, England); X-ray powder diffraction (XRD) patterns of nanoparticles over the 2θ range of 5 to 50° were recorded on a Rigaku Miniflex II diffractometer using Cu-Kα radiation at a scan speed of 5°/min. Fourier transform infrared spectra (FT-IR) were scanned over the range of 400-2000 cm^{-1} on an IR Affinity-1 spectrometer (Shimadzu, Japan). UV-vis absorption spectra were measured by a UV 2450 spectrophotometer (Shimadzu, Japan).

DFT calculations

The projected augmented wave method (PAW) was employed to describe the electron-ion interactions. The exchange-correlation energies were depicted using the Perdew-

Burke-Ernzerhof scheme within the generalized gradient approximation (PBE-GGA). A plane-wave energy cutoff was set at 500 eV, and the convergence criteria for total energy and force were 10^{-5} eV and 0.02 eV/Å, respectively. The Brillouin zone sampling was conducted using a 1 × 1 × 1 Monkhorst-Pack k-point grid. To accurately reflect the repulsive or attractive interactions between reactant molecules and the ZIF framework, the DFT-D3 method with Becke-Jonson damping was used for van der Waals dispersion correction during structural optimization and energy calculations. After fully optimizing all structures using PBE-D3, energy level calculations were performed. First, self-consistent field (SCF) calculations were conducted to obtain the ground-state electron density of the system. Then, non-self-consistent field (NSCF) calculations were performed based on this electron density. During the calculations, a high-density k-point grid was employed for Brillouin zone sampling to ensure the accuracy of the energy level calculations. Finally, VASPKIT was used to analyze the density of states (DOS) distribution near the Fermi level.

Synthesis of ZIF-90

Zinc acetate methanol solution (30 mM, 1.5 mL) was heated to 65 ℃ and stirred for 1 h. It was then dripped into 2-methylimidazole methanol solution (90 mM, 4.5 mL). The mixture was stirred for 30 min and then centrifuged at 7000 rpm. The precipitate was washed three times with ethanol and deionized water, and dispersed in deionized water for further use.

Synthesis of ZIF-90@Dyes

The diameter of the micropores of ZIF-90 is less than 0.6 nm.[1,2] The sizes of fluorescent dyes (e.g., 6-FAM and Cy5) are considerably larger than the pore size of ZIF-90. Therefore, instead of Cy5 or 6-FAM, a single-stranded DNA modified with Cy5 or 6-FAM was utilized to prepare ZIF-90@Dyes. The electrostatic and π-π stacking interactions between the single-stranded DNA and ZIF-90 can enhance the binding affinity between the fluorescent molecules and ZIF-90,[3,4] and hence enable the immobilization of fluorescent molecules on the surface of ZIF-90.

ZIF-90@Dyes (i.e., ZIF-90@Cy5 or ZIF-90@FAM) was prepared according to

the following protocol. Briefly, DNA-Cy5 or DNA-FAM (15 μL, 100 μM) was mixed with ZIF-90 (200 μL, 4 mg/mL) and oscillated for 12 hours on a 200 r/min horizontal oscillator. After centrifugation, the precipitate was washed three times with deionized water, dispersed in deionized water, and stored in a refrigerator at 4 °C.

Detection of ATP in both aqueous solutions and cell lysates using either ZIF-90 or ZIF-90@Cy5

A series of working standard solutions with different ATP concentrations were obtained by diluting the ATP stock solution with appropriate amounts of deionized water. For each of the three cell lines (i.e., 293T, MCF-7, and A549), the same number of cells were lysed by repeated freeze-thaw cycles. The resulting cell lysates were diluted 20-fold (approximately 5×10^3 cells/mL) for subsequent analysis. To 200 μL of each sample (either working standard solutions or cell lysates), 2 μL of either ZIF-90 or ZIF-90@Cy5 (4 mg/mL) was added and thoroughly mixed. In addition, ZIF-90@FAM is added 5 folds as much as ZIF-90@Cy5 (10 μL, 4 mg/mL). The mixture was allowed to react for 2 min, and then subjected to fluorescence measurements on an F7000 fluorescence spectrophotometer (Hitachi, Japan) equipped with a continuous xenon arc lamp.

Fluorescence imaging of ATP in cells using either ZIF-90 or ZIF-90@Cy5

Cell lines (e.g., MCF-7, HeLa, MCF-10A) were firstly cultured in Dulbecco's modified eagle medium (DMEM) medium for 24 hours in the presence of 5% CO_2 at 37°C, and subsequently incubated at 37°C for 8 hours in culture medium containing 0.5 mg/mL of either ZIF-90 or ZIF-90@Cy5. After being washed three times with PBS, they were incubated with 1 mL of Hoechst 33342 solution (0.1 mg/mL) for 20 min. After another three rounds of PBS washing, cells were finally subjected to image acquisition by a Nikon Ti-E+ A1R MP confocal S-2 laser scanning fluorescence microscope (Nikon, Japan) using a 60× oil dipping objective

The estimation of the limit of detection

The limit of detection (LOD) value is estimated according to the following equation:

$LOD = 3\sigma/S$

Where σ is the standard deviation of the blank solution, and *S* is the slope of the calibration curve established between the fluorescence intensity and the concentration of the analyte of interest.

References

1. M. Li, J. Liu, S. Deng, Q. Liu, N. Qi and Z. Chen, *ACS Appl. Energy Mater.*, 2021, **4**, 7983-7991.
2. H.L. Hung, T. Iizuka, X, Deng, Q. Lyu, C.H. Hsu, N. Oe, L.C. Lin, N. Hosono and D.Y. Kang, *Sep. Purif.*, 2023, **310**, 123115.
3. S. Wang, R. Wang, D. Jiang, N. Zhang and W. Jiang, *Sensor Actuat. B-Chem.*, 2022, **357**, 131400.
4. G. Wang, T. Cheng, H. Yuan, F. Zou, P. Miao and J. Jiao, *Biosens. Bioelectron.*, 2023, **228**, 115226.

Tables and Figures

Table S1. Distributions of elements in ZIF-90 calculated from its EDS measurements

Elements	Wt±Stand deviation %	Atomic%
C	42.03	55.88
N	22.14	25.24
O	12.77	12.75
P	1.49	0.77
S	0.38	0.19
Zn	21.19	5.18
Total	100.00	100.00

Table S2. The sequences of DNA strands used in the experiments

Strands	Sequences (from 5' to 3')
DNA-Cy5	TAGCTTATCAGACTGATGTTGA-Cy5
DNA-HEX	TAGCTTATCAGACTGATGTTGA-HEX
DNA-FAM	TAGCTTATCAGACTGATGTTGA-FAM

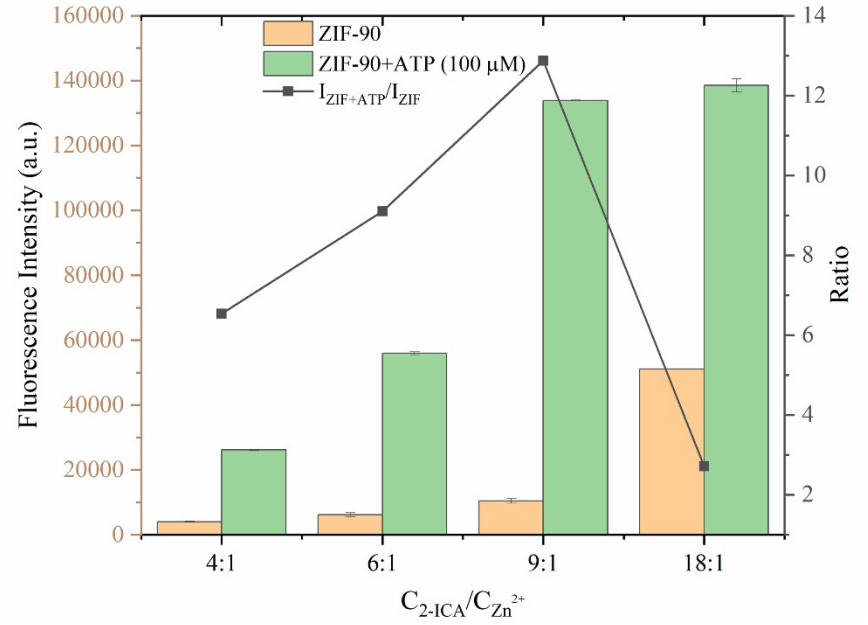

Figure S1. The fluorescence responses of ZIF-90 prepared with different concentration ratios between 2-ICA and Zn^{2+}.

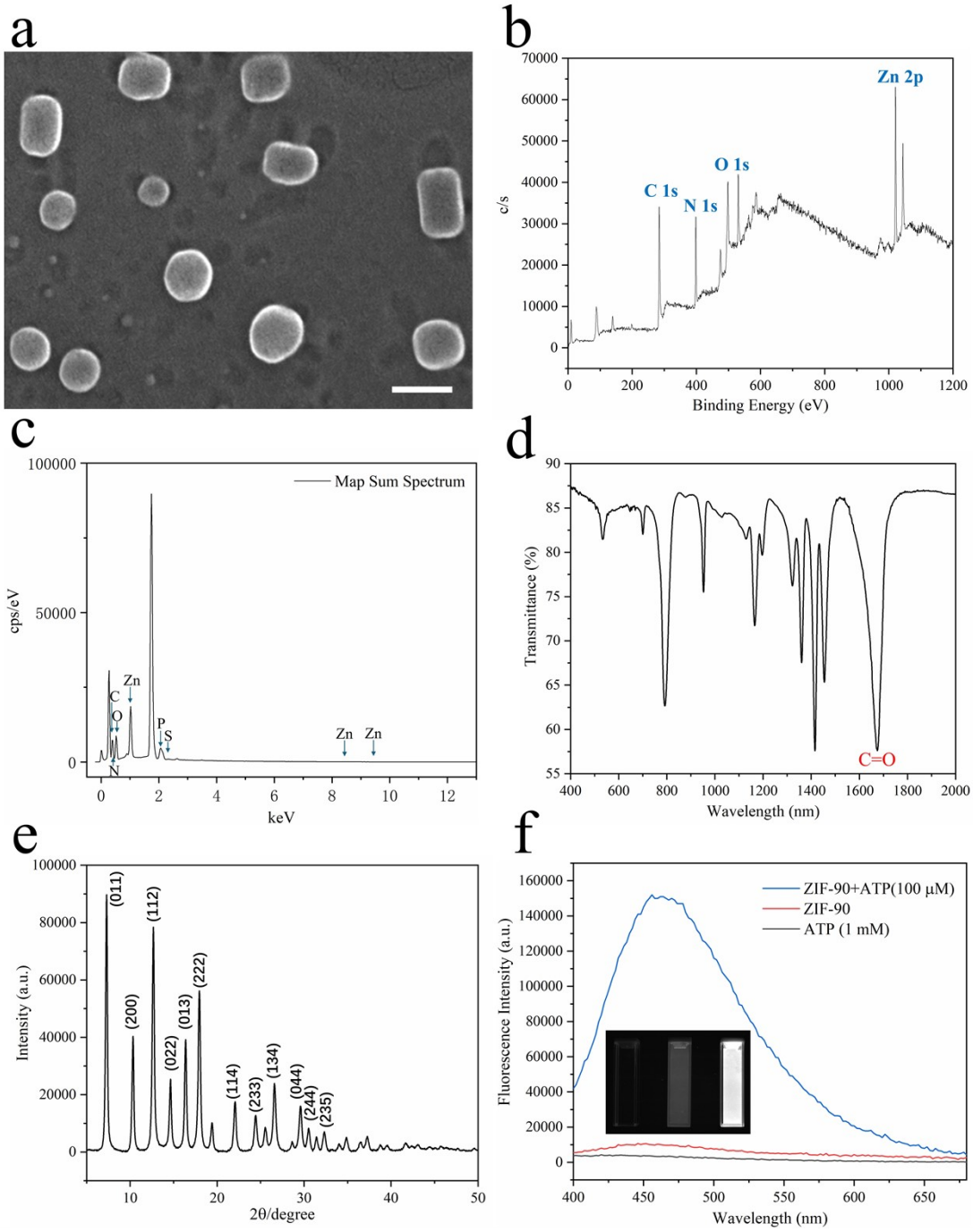

Figure S2. a, b, c, d and e: the SEM image (Scale bar: 100 nm), XPS measurements, EDS measurements, FT-IR spectrum and XRD profile of ZIF-90; f: the fluorescence spectra and of ZIF-90, ZIF-90+ATP (100 μM) and ATP (1 mM) under UV light (365 nm) irradiation, respectively. Photographs of 100 μM ATP (left), ZIF-90 (middle) and ZIF-90+100 μM ATP (right) are inserted.

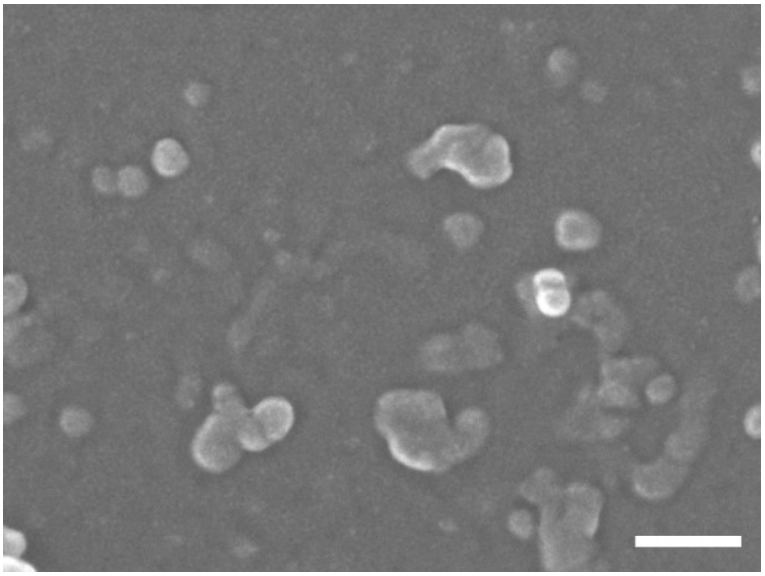

Figure S3. SEM image of mixture of 200 μL ZIF-90 (0.1 mg/mL) and 100 μM ATP (Scale bar: 100 nm).

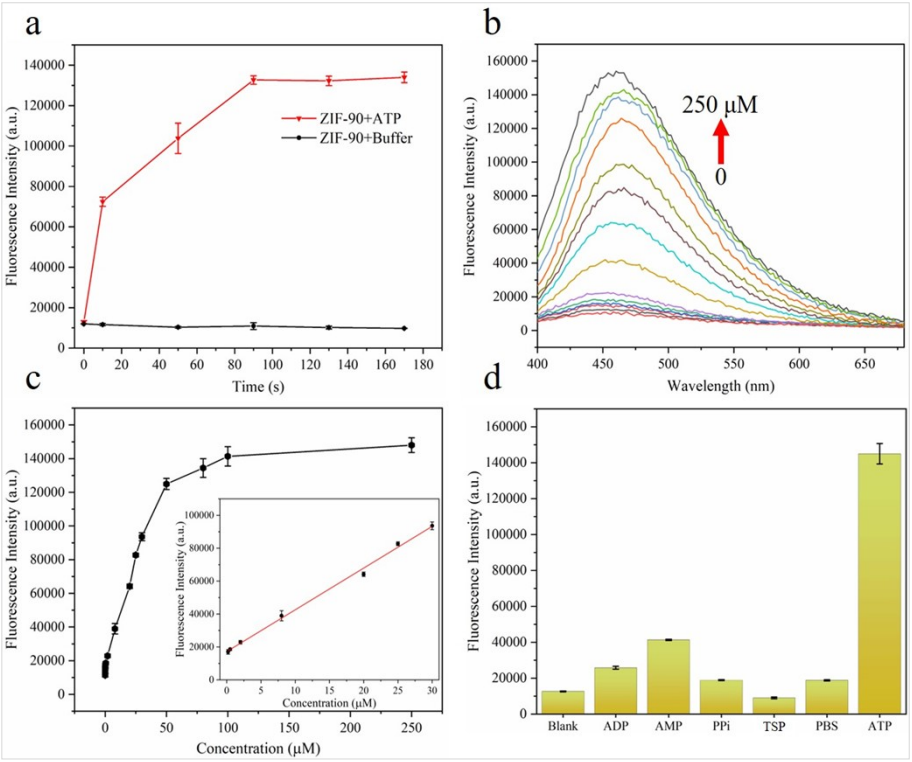

Figure S4. a) the fluorescence responses of ZIF-90 to buffer and ATP (100 μM) measured during different time periods, respectively; b) Fluorescence responses of ZIF-90 to samples with different ATP concentrations (0-250 μM); c) Relationship between the fluorescence response of ZIF-90 at 458 nm and ATP concentrations within the range of 0-250 μM; d) The fluorescence responses of ZIF-90 to ATP, ADP, AMP, PPi, TSP, and PBS buffer, respectively (the concentrations of these species were all 100 μM).

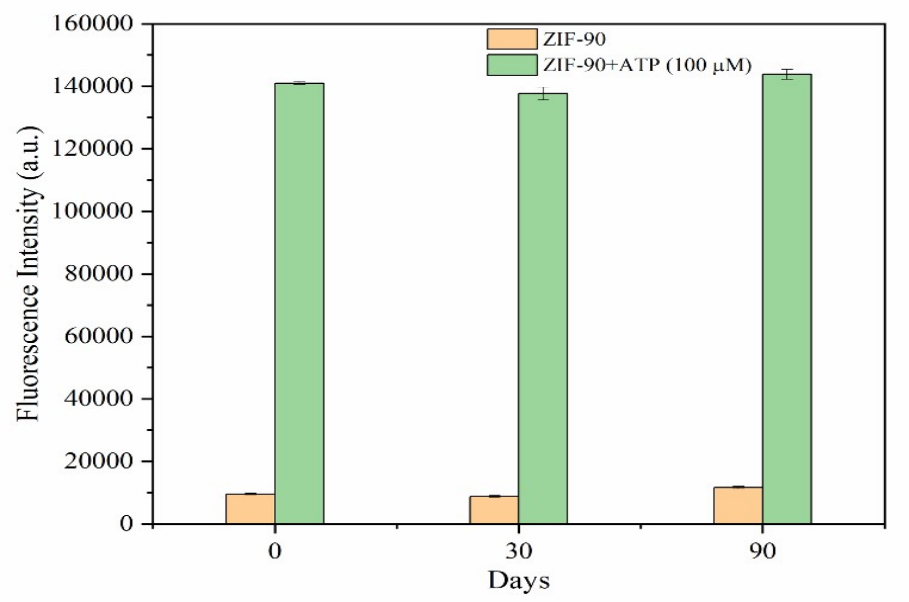

Figure S5. Fluorescence responses of ZIF-90 after being stored for different periods of time.

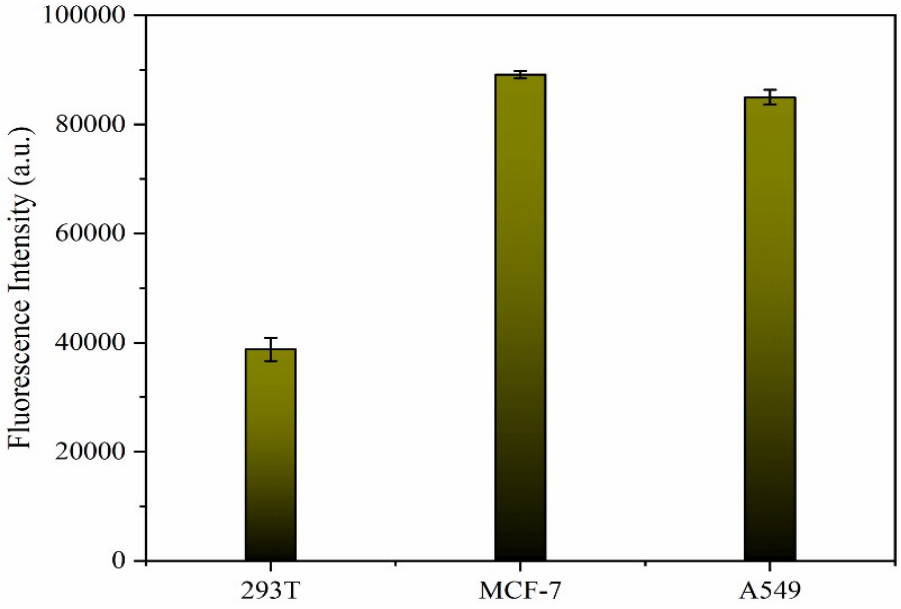

Figure S6. Fluorescence responses of ZIF-90 to different cell lysates.

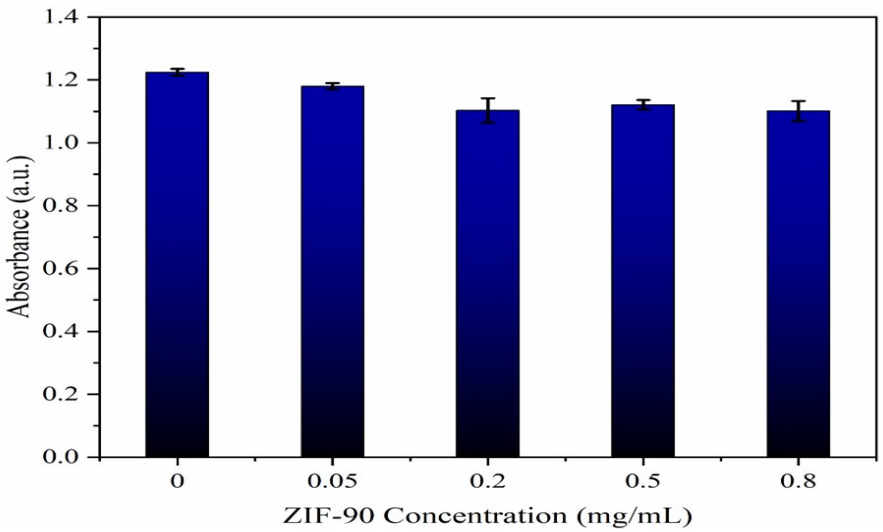

Figure S7. Absorbance of MTT Formazan at 490 nm for Hela cells cultured in culture medium containing different concentrations of ZIF-90.

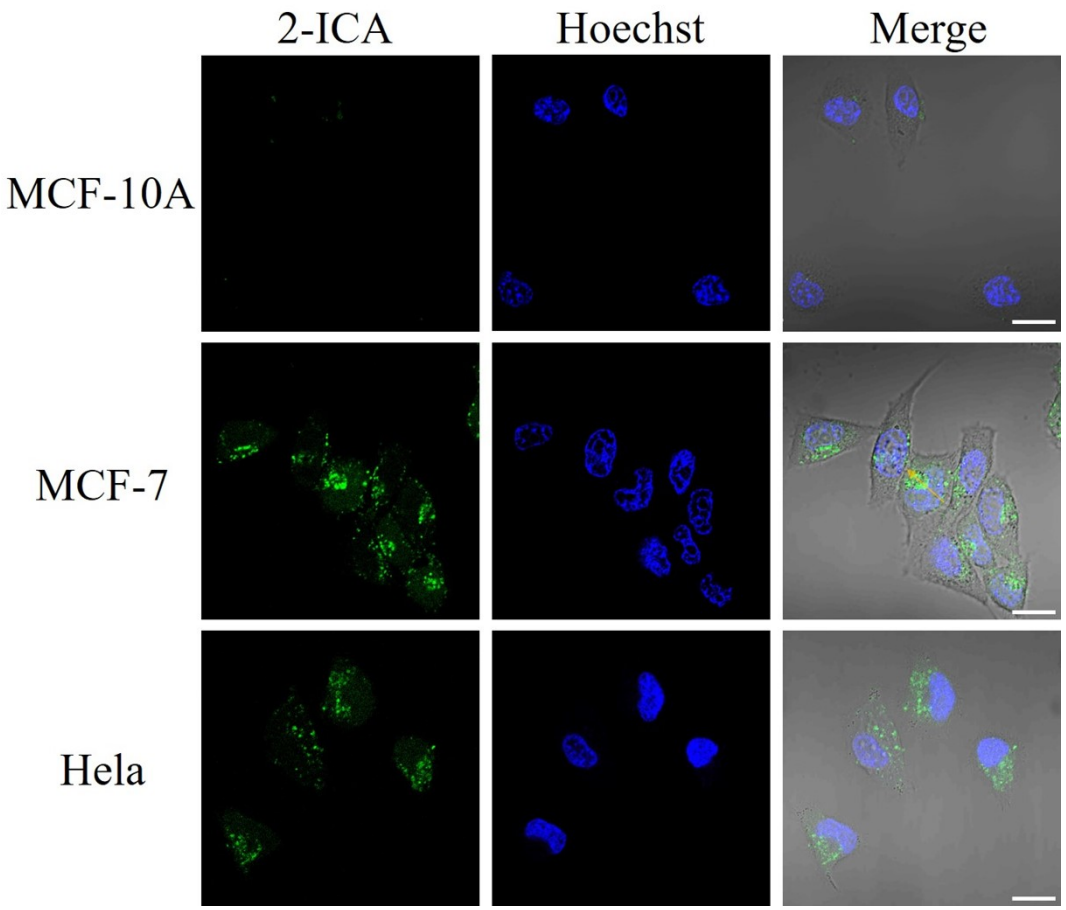

Figure S8. Confocal laser scanning microscopic images of different cells (MCF-10A, MCF-7, HeLa) after incubated with ZIF-90 (Scale bar: 20 μm).

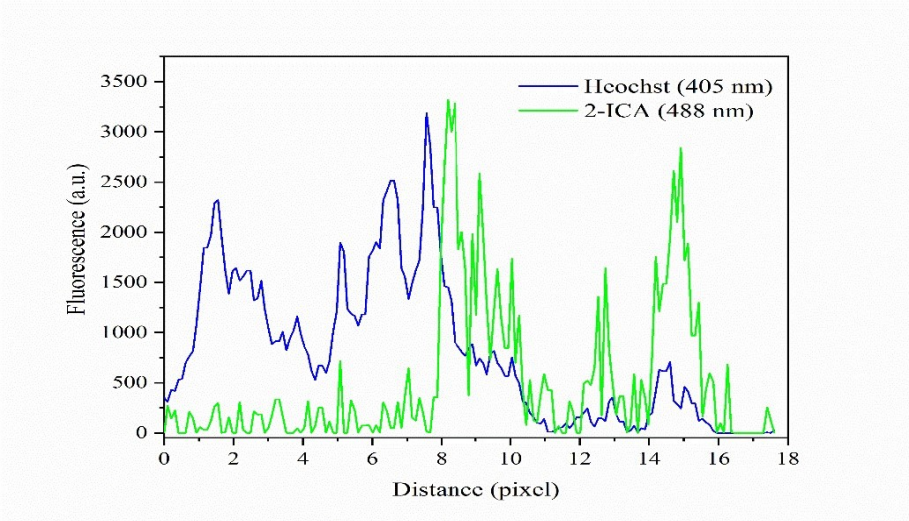

Figure S9. Fluorescence intensities measured at the two wavelength channels (i.e., 405 and 488 nm) along the orange arrow in the image of MCF-7.

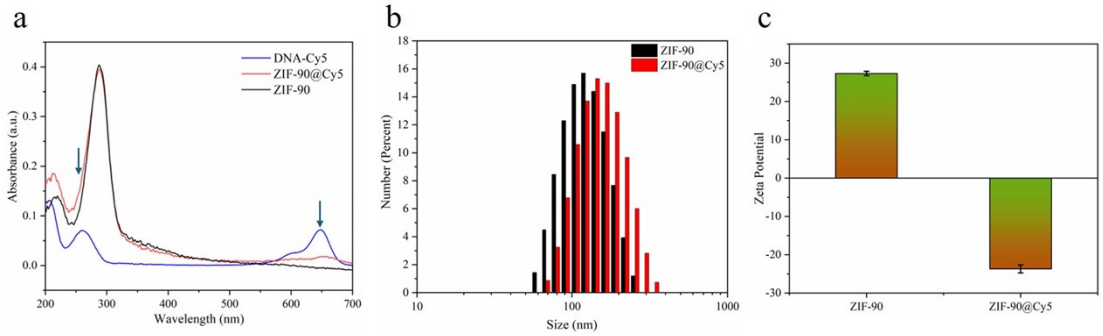

Figure S10. a) UV-Vis spectra of ZIF-90, ZIF-90@Cy5, and Cy5 solutions; b) DLS measurements and zeta potential distributions (c) of ZIF-90 and ZIF-90@Cy5.

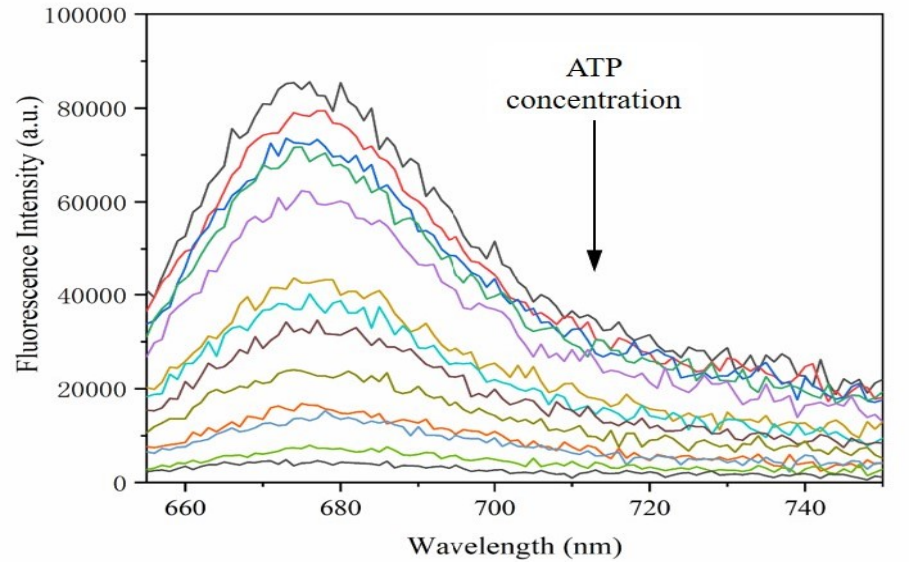

Figure S11. Fluorescence spectra of ZIF-90@Cy5 after being treated with different concentrations of ATP (0-500 μM).

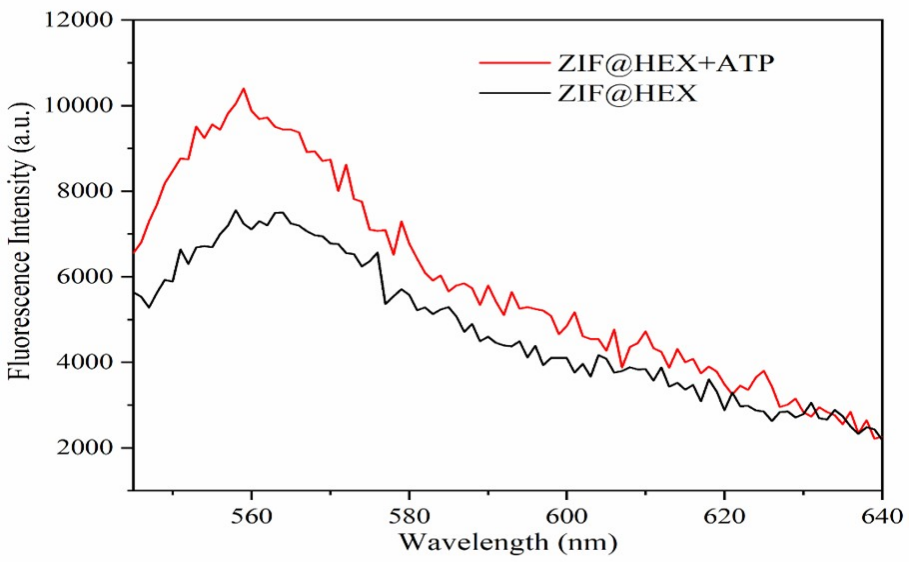

Figure S12. The fluorescence spectra of ZIF-90@HEX and its mixture with ATP (100 μM).

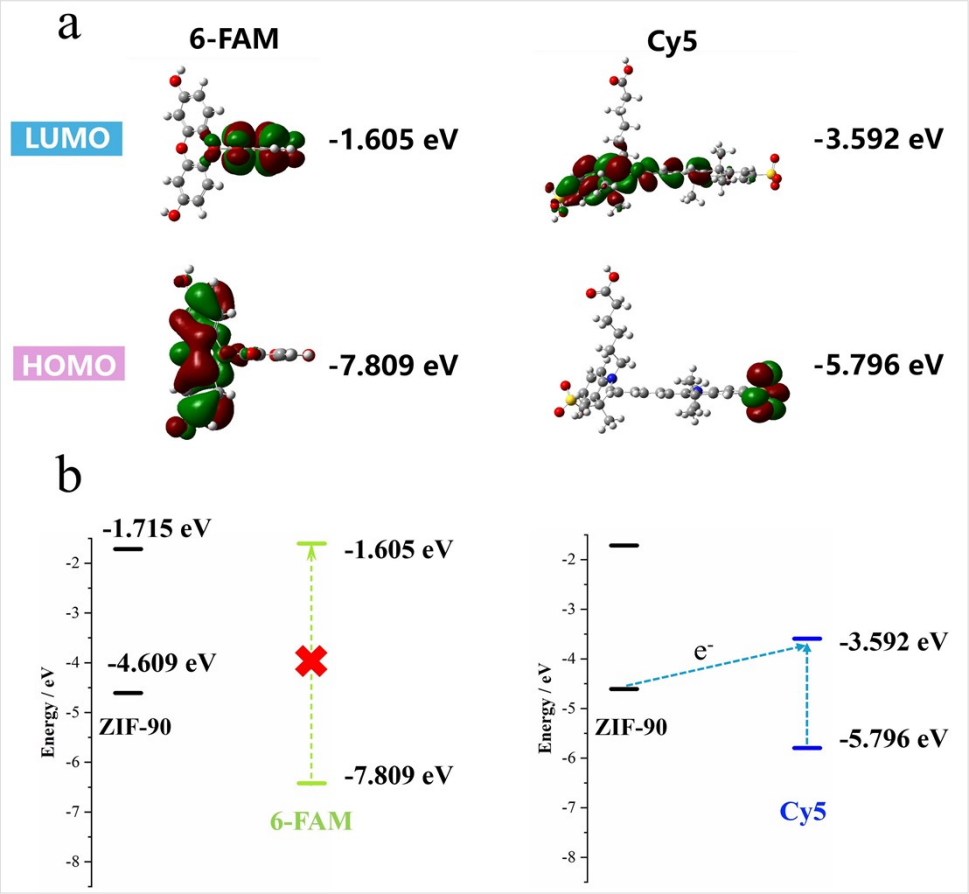

Figure S13. a) Distributions of the electronic states in the HOMO and LUMO of 6-FAM and Cy5, respectively; b) Charge transfer mechanisms between ZIF-90 and fluorescence dyes (i.e., Cy5 and 6-FAM).

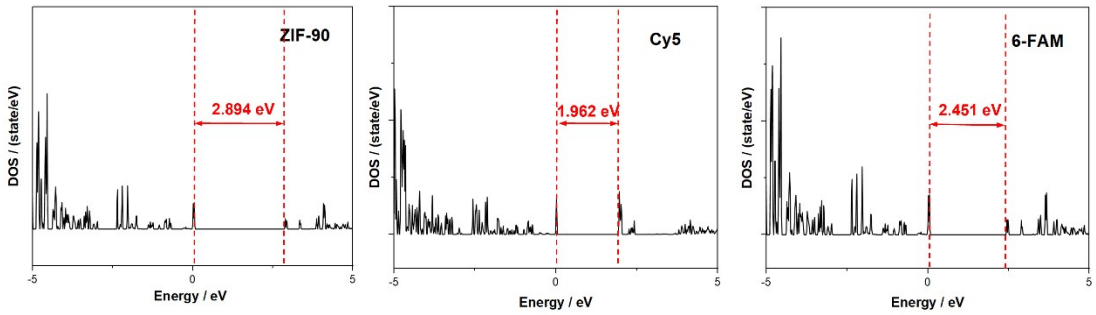

Figure S14. The energy levels of ZIF-90, and the two fluorescent dye molecules (i.e., Cy5 and 6-FAM) in their free states.

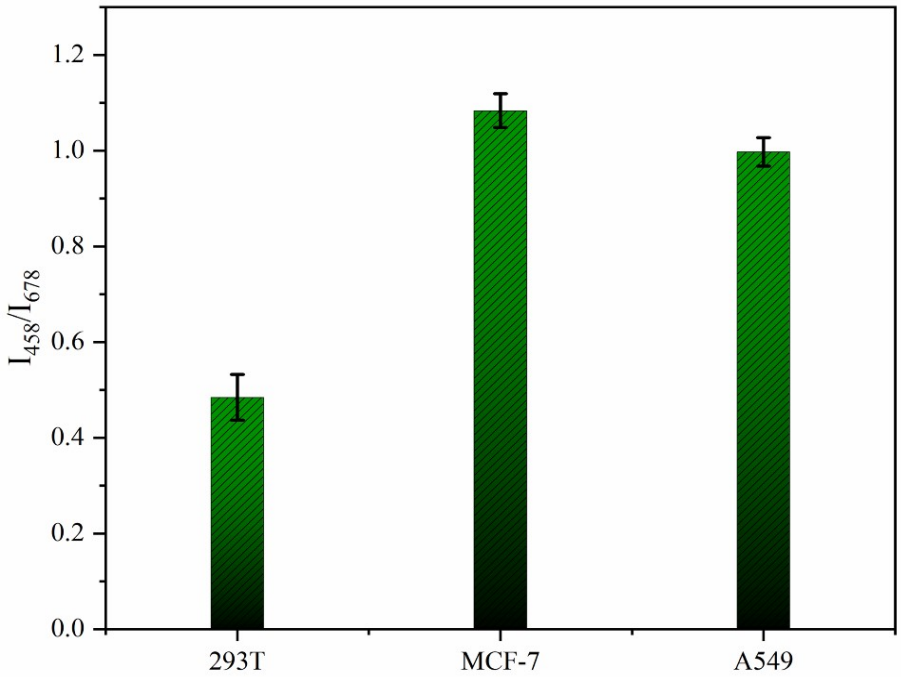

Figure S15. Fluorescence responses of ZIF-90@Cy5 to different cell lysates.